Science Journal of Chemistry
2024, Vol. 12, No. 3, pp. 54-62
https://doi.org/10.11648/j.sjc.20241203.12

Research Article

3-Sphere Tetrahedral Angles and Phase Angle of the Pseudorotation P[deg] of C_1-CH_3-α-D Ribitol Iminocyclitol

Petru Filip, Carmen Irena Mitan*, Emerich Bartha

Department of Chemistry, "C. D. Nenitescu" Institute of Organic and Supramolecular Chemistry, Bucharest, Romania

Abstract

3-Sphere dihedral angles θ_{HnHn+1}[deg] calculated from NMR data, from vicinal coupling constant $^3J_{HnHn+1}$[Hz] with right sign and stereochemistry, are used for simulation of the conformation of the five membered ring with VISION molecular models and Gausian09W. For a vicinal angle ϕ[deg], angle result from vicinal coupling constant $^3J_{HnHn+1}$[Hz], result three possible dihedral angles with negative and positive sign. Different phase angles of the pseudorotation results from combination of dihedral angles (exocyclic angles) with positive and negative sign in case of *cis* stereochemistry, and only negative sign for *trans* stereochemistry, in accord with D-ribitol stereochemistry. The sign of the endocyclic *trans-ee* torsional angle is positive, relative to *trans-aa* and *cis* stereochemistry with same sign as exocyclic angle, as visualized on VISION molecular models. Tetrahedral angles φ_{Cn}[deg] in close relationship with dihedral angles θ_{HnHn+1}[deg] are calculated only from vicinal coupling constant $^3J_{HnHn+1}$[Hz] in attempt to corelate the change in conformation with tetrahedral values φ_{Cn}[deg] and bond lengths l[A^0], once the iminocyclitol push out from planarity one or two atoms of carbon, and once again to confirm the method for calculation of tetrahedral angles of five membered ring, sin/tan *versus* sin/cos units.

Keywords

3-Sphere, Dihedral Angle, Tetrahedral Angle, Vicinal Angle, Vicinal Coupling Constant, C_1-CH_3-α-D-Ribitol, Conformational Analysis

1. Introduction

Conformational analysis on five and six membered rings with biological activity (*i.e.* antiviral activity) as a pseudorotation concept appears around 1947, thermodynamic studies on cyclopentene conformation performed by Kilpatrich, Pitzer si Spitzer [1] and Pitzer si Donath [2]. First spectroscopical evidence was obtained in 1965 on far infrared of tetrahydro furan [3]. Cremer and Pople [4] used this model in calculation of the conformation of carbasugar, and Altona [5] in vitamin D five membered ring or nucleic acid conformation.

Recently are published results based on 1H NMR, DFT and X-ray data for determination of the conformation of furanose substrates with restricted freedom of rotation on the C_3-C_4, C_2-C_3, and C_1-C_2 bonds [6], known as antivirale, antibacteriene or anticancer. *i.e.* Molnupiravir approve by WHO (World Health Organization) in treatment of COVID-19 [7]. Optimization of the geometry in case of *N*-(α-D-glucofuranurono-6, 3-lactone) and *N*-(methyl β-D-glucopyranuronate)-p-nitroanilines was realized with DFT (B3YPP/6-311+G++ method), and structures are

*Corresponding author: cmitan@yahoo.com.com (Carmen Irena Mitan)

Received: 16 May 2024; **Accepted:** 3 June 2024; **Published:** 19 June 2024

simulated with MOLDEN program and all calculation with Gaussian 03. [8]

Our aim is to state a general method for calculation tetrahedral angles φ_{Cn}[deg] with 3-Sphere approach in close relationship with dihedral angles θ_{HnHn+1}[deg], analyzing the phase angle of the pseudorotation. Three dihedral angles θ_{HnHn+1}[deg] are calculated for every vicinal coupling constant $^3J_{HnHn+1}$[deg], and only for *trans* θ_{H3H4}[deg] dihedral angle the sign is resticted by D-ribitol stereochemistry.

2. Conformational Analysis

Conformational analysis, [9, 10] phase angle of the pseudorotation P[deg] (eq. 1) and angle of deviation from planarity θ_m[deg] (eq. 2) calculated with 3-sphere dihedral angles θ_{HnHn+1}[deg] and Altona formalism are published already [11].

$$P = \tan^{-1}\frac{(\theta_{H2H4}+\theta_{H1N})-(\theta_{H1H2}+\theta_{H4N})}{\theta_{H2H3}(\sin 72 + \sin 144)} \quad (1)$$

$$\theta m = \frac{\theta 0}{cosP} \quad (2)$$

Where: P – pahase angle of pseudorotation [deg], θ_m – angle of deviation from planarity[deg], θ_{HnHn+1} – 3-Sphere dihedral angles[deg].

2.1. Endocyclic Torsional Angles

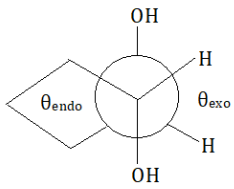

$\theta_{exo} = A + B\theta_{endo}$
cis: A=1, B=0, *trans:* A=1, B=120

Figure 1. *Exocyclic (dihedral angles) and endocyclic torsional angles.*

Endocyclic angle θ_{endo}[deg], an angle at intersection of l_{Cn-1Cn} and $l_{Cn+1Cn+2}$[A^0] along the bond length l_{CnCn+1}[A^0] (Figure 1), in case of polynomial equations in close relationship with corresponding exocyclic angle θ_{exo}[deg] gives the PSEUROT program, [12] endocyclic angles θ_{endo}[deg] are usefully on Altona model. [11] Endocyclic torsional angles (Figure 1) calculated with PSEUROT equations for D-ribose (Eq. 3-5) [12]:

$$\theta_{endoH1H2} = 0.9090x\ (\theta_{exoH1H2} - 3.3) \quad (3)$$

$$\theta_{endoH2H3} = 0.9174x\ (\theta_{exoH2H3} - 0.2) \quad (4)$$

$$\theta_{endoH3H4} = 0.9090x\ (\theta_{exoH3H4} + 124.9) \quad (5)$$

Other posibility under reflexion for calculation of the endocyclic torsional angles θ_{endo}[deg] can be: 3-sphere dihedral angle θ_{HnHn+1}[deg] divided with vicinal coupling constant $^3J_{HnHn+1}$[Hz] (eq. 6) in case of *cis*, *trans-aa* stereochemistry or multiplaid with vicinal coupling constant $^3J_{HnHn+1}$[Hz] (eq. 7, 8) in case of *trans-ee* stereochemistry, in line with polar equations. That must be confirmed by NMR data and X-ray. As observation eq. 8 gives too smaller endocyclic angles betwwen 0.1 and 0.5[Hz] for n = 2, angles result sometimes from simulation with Gausian09W. In case of *trans-ee* stereochemistry the exocyclic angle transformed in endocyclic torsional angle (eq. 16) with corresponding sign can be also contemplate. In this light for *trans-aa* stereochemistry also the 120 rule must be used (eq. 18). On molecular models with an angle of 120[deg] between H_1 - OH_1 and H_2 - OH_2 the ring of iminocyclitol is plane, any modification with required number of degrees between H_1 and H_2 must be proportional with endocyclic angle.

$$cis\text{-}ae,\ trans\text{-}aa\text{:}\ \theta_{endo} = \theta_{HnHn+1}/^3J_{HH} \quad (6)$$

$$trans\text{-}ee\text{:}\ \theta_{endo} = (\theta_{HnHn+1}{}^{trans\text{-}ee} x\, ^3J_{HH})/2 \quad (7)$$

$$trans\text{-}ee\text{:}\ \theta_{endo} = (\theta_{n,n+1\ x}\ ^3J_{HH})/n \quad (8)$$

Where θ_{endo} – endocyclic torsional angle [deg], θ_{HnHn+1} – dihedral angle or exocyclic angle [deg], $\theta_{n,n+1}$ – exocyclic torsional angle [deg].

3-Sphere dihedral angles are calculated (eq. 9-13) from vicinal angle (eq. 14) an angle calculated from vicinal coupling constant. [13]

$$cis,\ trans\text{-}ee^{3,\ 2}\text{:}\ \sin^{-1}\cos\phi = \theta_{HnHn+1} \quad (9)$$

$$trans\text{-}aa^{6,\ 1\ or\ 5,\ 2},\ trans\text{-}ee^{4,\ 1}\text{:}\ \cos^{-1}\sin(-\phi) = \theta_{HnHn+1} \quad (10)$$

$$\tan^{-1}\sin(-\phi) = \theta_{HnHn+1} \quad (11)$$

$$\sin^{-1}[\cot(-\phi)] = \theta_{HnHn+1} \quad (12)$$

$$\sin^{-1}[\tan(-\phi)] = \theta_{HnHn+1} \quad (13)$$

$$\phi = (nx^3J_{HnHn+1})^2 \quad (14)$$

Where: θ_{HH}[deg] – dihedral angle, ϕ[deg] – vicinal angle, $^3J_{HH}$[Hz] – vicinal coupling constant, with *cis*, *trans-ee*: m = 2, *trans-aa*: m = 1.

The relationship between the 3-Sphere dihedral angles with *cis* and *trans* stereochemistry was established based on Hopf fibration trigonometric equations applaid on six angles with *cis* and *trans-ee* and *trans-aa* stereochemistry (eq. 15-17), [14] totaly in contradiction with Karplus 120 rule (eq. 18).

$$trans\text{-}aa^{6,\ 1\ or\ 5,\ 2}\text{:}\ \theta_{HnHn+1}{}^{cis} = 180 - \theta_{HnHn+1}{}^{trans} \quad (15)$$

$$trans\text{-}ee^{4,\ 1\ or\ 3,\ 2}\text{:}\ \theta_{HnHn+1}{}^{cis} = 120 - \theta_{HnHn+1}{}^{trans} \quad (16)$$

$$trans\text{-}ee^{4,\,1\ or\ 3,\,2}: \theta_{HnHn+1}{}^{trans} = -90 \text{ -/+ } \theta_{HnHn+1}{}^{cis} \quad (17)$$

$$\theta_{n,n+1} = 120 - \theta_{HnHn+1} \quad (18)$$

Where θ_{HnHn+1} – 3-Sphere dihedral angle with *cis*, *trans-ee* and *trans-aa* stereochemistry, θ_{endo} – endocyclic torsional angle.

The main question, 120 rule is applaid in case of endocyclic torsional angles only for *trans* stereochemistry? In this case the torsional angle of *trans-aa* dihedral angle -167.13[deg] is -47.13[deg] instead -12.87[deg], realtive to -18.99[deg] result from eq. 6 (Table 2). In case of dihedral angle with *cis* stereochemistry of 51.56[deg] the torsional angle is 8.44[deg] under 120 rule (eq. 18), realtive to 16.63[deg] result from eq. 6. In case of *cis* stereochemistry PSEUROT program (eq. 3, 4) shown smaller differences, no more as 3[deg]. [12]

2.2. Relationships Between Phase Angle of the Pseudorotation and Other Physical Coordinates

The angle of deviation from planarity can be calculated from the phase angle of the pseudorotation P[deg] with Altona equation eq. 2 from θ_{H2H3} or with eq. 19, 20 from θ_{H1H2} or θ_{H3H4}[deg]. [11]

$$\theta_m = \theta_{H1H2}/\cos (P - 144) \text{ [deg]} \quad (19)$$

$$\theta_m = \theta_{H3H4}/\cos (P + 144)\text{[deg]} \quad (20)$$

The atom coordinate, the out-of plane vibrations Zj calculated with Levitt methods (eq. 21).[15]

$$Zj = (2/5)^{1/2} x q_m x \cos (P + jx144 - 90),\ j\ 0 - 4 \quad (21)$$

Where: Z_j out-of plane vibrations, q_m – amplitude [A^0] calculated from endocyclic torsional angle θ_{endo}[deg], P – phase angle of the pseudorotation [deg].

Grabb – Harvey relationships (22-27) for calculation torsional constraints ν^0[deg] from phase angle of the pseudorotation P[deg] and q_m[A^0] [16].

$$\nu^0 = q_m \cos (P + 72) \quad (22)$$

$$\nu^1 = -q_m \cos (P + 36) \quad (23)$$

$$\nu^2 = q_m \cos (P) \quad (24)$$

$$\nu^3 = -q_m \cos (P - 36) \quad (25)$$

$$\nu^4 = q_m \cos (P - 72) \quad (26)$$

$$\nu^0 + \nu^1 + \nu^2 + \nu^3 + \nu^4 = 0 \quad (27)$$

Bartenev – Kameneva – Lipanov relationship for calculation of the tetrahedral angles φ_i[deg] from phase angle of pseudorotation P[deg] (Eq. 28-35). [17]

$$\varphi_i = A_i + B_i x \cos (2P - 72i + ci) \quad (28)$$

$$\varphi_0 = 108.8 + 1.4\cos (2P - 0x75 - 10) \quad (29)$$

$$\varphi_1 = 105.2 + 0.8\cos (2P - 1x75 + 16) \quad (30)$$

$$\varphi_1 = 106.6 + \cos (P) \quad (31)$$

$$\varphi_2 = 103.5 + 1.5\cos (2P - 2x75 - 36) \quad (32)$$

$$\varphi_3 = 102.9 + 1.6\cos (2P - 3x75 + 9) \quad (33)$$

$$\varphi_4 = 106.2 + 1.1\cos (2P - 4x75 + 8) \quad (34)$$

$$\varphi_4 = 105.3 - (P) \quad (35)$$

The relationship between proton-proton torsional angle φ [deg] and the pseudorotational parameters P[deg] and q_m[A^0] for ${}^3J_{2,3}$[Hz] extracted from X-ray data (eq. 36) [18].

$${}^3J_{2,3}(ribo): \varphi_{2,3} = 0.2 + 1.09 q_m \cos P \quad (36)$$

2.3. Bond Lengths l_{CnCn+1}[A^0]

The bond lengths [19] can be calculated with eq 37 using the theoretic carbon-carbon bond length distance (l_0 = 1.54[A^0]) with results equals [20] with a method for calculation published by Maksic and Randic [21]. Recently, based on dihedral angle under wave theory the proton-proton bond lengths l_{HnHn+1}[A^0] was calculated without theoretic bond distance (results presented elsewhere). Thus, probably the eq. 37 can be reconsidered, eq. 38 for calculation carbon-carbon bond length distance l_{CnCn+1}[A^0] without the theoretic bond length giving comparable results.

$$l_{CnCn+1} = [l_0 x 1.57 x \cos^{1/2}(\theta/m)]^{1/2} [A^0] \quad (37)$$

$$l_{CnCn+1} = 1.57 x \cos^{1/4}(\theta^{cis}/n) [A^0] \quad (38)$$

Where l_{CnCn+1} - carbon-carbon bond length distance [A^0], l_0 - theoretic carbon-carbon bond length distance [A^0], n = 1 for *cis*[6,1] and *trans-aa*[6,1], *trans-ee*[4,1] – transformed in *cis*, n = 2 for *cis*[5,2] and *trans-aa*[5,2], *trans-ee*[3,2] – transformed in *cis*, alternatively n = 4 for *trans-ee*.

Meyer et. al reported a model for calculation the bond length from pseudorotation angle P[deg] (Eq. 34-36). [22]

$$r_{(C2-C3)} = r_{cc}{}^{(0)} + r_{cc}{}^{(2)} \cos 2P \quad (39)$$

$$r_{(C1-C2)} = r_{cc}{}^{(0)} [1 + \varepsilon_{lp} \cos 2P] + r_{cc}{}^{(2)} \sin 2P \quad (40)$$

$$r_{(C3-C4)} = r_{cc}{}^{(0)} [1 + \varepsilon_{lp} \cos 2P] - r_{cc}{}^{(2)} \sin 2P \quad (41)$$

where $r_{CC}{}^{(0)}$ = 1.537[A^0], $r_{CC}{}^{(2)}$ the C-C bond extension due

to the repulsion of the eclipsed vicinal C-H bonds, εlp the effect of the lone electron pairs of the oxygen.

3. Materials and Methods

Gausian09W [23], VISION molecular models [24].

3-Sphere approach for calculation of the dihedral angles θ_{HnHn+1}[deg], tetrahedral angles φ_{Cn}[deg], and bond lengths l_{CnCn+1}[A^0], using Hopf fibration and Lie algebra, trigonometric equations and algebraic equations. [25]

4. Results

3-Sphere dihedral angles θ_{HnHn+1}[deg] calculated from vicinal coupling constant $^3J_{HnHn+1}$[Hz] are used for simulation of the phase angle of the pseudorotation [10] and analyzed the tetrahedral angles in close relationship with dihedral angles (Table 1) with Bartenev – Kameneva – Lipanov [17] tetrahedral angles φ[deg] calculated from phase angle of the pseudorotation (Table 2).

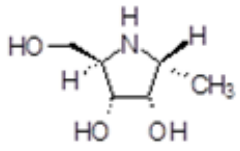

1

Figure 2. *Iminocyclitol 1 with C_1-methyl-α-D ribitol stereochemistry.*

Table 1. *Tetrahedral angles φ_{Cn}[deg] in close relationship with dihedral angles θ_{HnHn+1}[deg] and vicinal angles ϕ[deg] calculated from vicinal coupling constant $^3J_{HnHn+1}$[Hz].*

Entry	$^3J_{HH}$[Hz][a] Φ[deg] θ_{HnHn+1} [deg]	A	B	C	D	E	F	G	$\varphi_{Cn} = f(\theta_{HnHn+1})$
1	3.1 38.44 51.56	21.56 38.44 81.56 98.44 141.56 158.44 *43.12* *8.439*	8.439 51.56 68.44 111.56 128.44 171.56 *16.879* *21.560*	16.87 43.12 76.88 103.12 136.88 163.12 *33.75* *13.12*	10.78 49.22 70.78 109.22 130.78 169.22 *21.56* *19.22*	19.22 40.78 79.22 100.78 139.22 160.78 *38.44* *10.78*	4.21 55.78 64.22 115.78 124.22 175.78 *8.439* *25.78*	25.78 34.22 85.78 94.22 145.78 154.22 51.56 4.21	$\sin^{-1}\cos 38.44 = 51.56\ \theta_{H1H2}$ $\cos^{-1}\sin(-38.43/2) = 109.22\ \varphi_{C1}$
2	3.1 38.44 -34.68 U to S ~ tan	25.31 34.68 85.32 94.68 145.32 154.68 *50.63* *4.68*	4.68 55.31 64.68 115.32 124.68 175.32 *9.36* *25.31*	9.36 50.63 69.36 110.64 129.36 170.64 *18.72* *20.63*	12.65 47.34 72.65 107.34 132.65 167.34 *25.31* *17.34*	17.34 42.65 77.34 102.65 137.34 162.65 *34.68* *12.65*	2.34 57.65 62.34 117.65 122.34 177.65 *4.68* *27.65*	27.65 32.34 87.65 92.34 147.65 152.34 *55.30* *2.34*	$\cos^{-1}\sin$-0.5x{ [60 – (98.44 – 90)]/1.5} = $\cos^{-1}\sin(-34.37/2) = 107.18\ \varphi_{C1}$
3	3.1 38.44 -31.86	28.13 31.86 88.13 91.86 148.13 151.86 *56.26* *1.86*	1.86 58.13 61.86 118.13 121.86 178.13 *3.73* *28.13*	3.73 56.26 63.73 116.26 123.73 176.26 *7.47* *26.26*	14.06 45.93 74.06 105.93 134.06 165.93 *28.13* *15.93*	15.93 44.06 75.93 104.06 135.93 164.06 *31.86* *14.06*	0.934 59.06 60.93 119.06 120.93 179.06 *1.86* *29.06*	29.06 30.93 89.06 90.93 149.06 150.93 *58.13* *0.93*	$\tan^{-1}\sin(-38.44) = -31.86\ \theta_{H1H2}$ $\cos^{-1}\sin(-31.86/2) = 105.93\ \varphi_{C1}$
4	3.1 38.44 -52.53	7.46 52.53 67.46	22.53 37.46 82.53	14.92 45.07 74.92	3.73 56.26 63.73	26.26 33.73 86.26	11.26 48.73 71.26	18.73 41.26 78.73	$\sin^{-1}\tan(-38.44) = -52.53\ \theta_{H1H2}$ $\sin^{-1}\cos(-52.53) = 37.46\ \theta_{H1H2}$ $\cos^{-1}\sin(-37.46/2) = 108.73\ \varphi_{C1}$

Entry	$^3J_{HH}$[Hz][a] Φ[deg] θ_{HnHn+1} [deg]	A	B	C	D	E	F	G	$\varphi_{Cn} = f(\theta_{HnHn+1})$
5	3.9 60.84 29.15	112.53 127.46 172.53 *14.92* *22.53* 0.84 59.16 60.84 119.16 120.84 179.16 *1.68* *29.15*	97.46 142.53 157.46 *45.07* *7.46* 29.15 30.84 89.16 90.84 149.16 150.84 *58.31* *0.84*	105.07 134.92 165.07 *29.85* *15.07* 1.68 58.31 61.68 118.32 121.68 178.32 *3.36* *28.31*	116.26 123.73 176.26 *7.46* *26.26* 0.42 59.58 60.42 119.58 120.42 179.57 *0.84* *29.58*	93.73 146.26 153.73 *52.53* *3.73* 29.58 30.42 89.58 90.42 149.57 150.42 *59.16* *0.42*	108.73 131.26 168.73 *22.53* *18.73* 14.57 45.42 74.58 105.42 134.57 165.42 *29.15* *15.42*	101.26 138.73 161.26 *37.46* *11.26* 15.42 44.58 75.42 104.58 135.42 164.57 *30.84* *14.57*	$\sin^{-1}\cos 60.84 = 29.15\ \theta_{H2H3}$ $\cos^{-1}\sin(-29.15/2) = 104.58\ \varphi_{C2}$
6	3.9 60.84 S to U ~ tan	19.72 40.28 79.72 100.28 139.72 160.28 *39.44* *10.28*	10.28 49.72 70.28 109.72 130.28 169.72 *20.56* *19.72*	20.56 39.44 80.56 99.44 140.56 159.44 41.12 9.43	9.86 50.14 69.86 110.14 129.86 170.14 19.72 20.14	20.14 39.86 80.14 99.86 140.14 159.86 40.28 9.86	5.14 54.86 65.14 114.86 125.14 174.86 10.28 24.86	24.86 35.14 84.86 95.14 144.86 155.14 49.72 5.14	$\cos^{-1}\sin$-0.5x{ [60 – (119.16 – 90)]/1.5} = $\cos^{-1}\sin(-20.56/2) = 100.28\ \varphi_{C2}$
7	3.9 60.84 -41.12	18.87 41.12 78.87 101.12 138.87 161.12 *37.74* *11.12*	11.12 48.87 71.12 108.87 131.12 168.87 *22.15* *18.87*	22.25 37.74 82.25 97.74 142.25 157.74 *44.51* *7.74*	9.43 50.56 69.43 110.56 129.43 170.56 *18.87* *20.56*	20.56 39.43 80.56 99.43 140.56 159.43 *41.12* *9.43*	5.56 54.43 65.56 114.44 125.56 174.43 *11.12* *24.43*	24.45 35.56 84.44 95.56 144.44 155.56 *48.8* *5.56*	$\tan^{-1}\sin(-60.84) = -41.12\ \theta_{H2H3}$ I. $\cos^{-1}\sin(-41.12/2) = 110.56\ \varphi_{C2}$ $\cos^{-1}\sin(-18.87/2) = 99.43\ \varphi_{C2}$ II. *$\cos^{-1}\sin[-(41.12 – 30)] = 101.12\ \varphi_{C2}$* *$\cos^{-1}\sin[-(41.12 – 18.87)/2] = 101.12\ \varphi_{C2}$*
8	3.9 60.84 -33.91	26.09 33.91 86.09 93.91 146.09 153.91 *52.19* *3.90*	3.90 56.09 63.91 116.09 123.91 176.09 *7.81* *96.69*	7.81 52.18 67.82 112.18 127.82 172.18 *15.63* *22.18*	13.04 46.95 73.04 106.95 133.04 166.95 *26.09* *16.95*	16.95 43.04 76.95 103.04 136.95 163.04 *33.91* *13.04*	1.95 58.04 61.95 118.04 121.95 178.04 *3.90* *28.04*	28.04 31.95 88.04 91.95 148.04 151.95 *56.09* *1.954*	$\sin^{-1}$[1/tan (-60.84)] = -33.91 θ_{H2H3} $\cos^{-1}\sin(-26.09/2) = 103.04\ \varphi_{C2}$
9	8.8 77.44 -167.13	12.87 47.12 72.87 107.12 132.87 167.12 *25.74* *17.12*	17.12 42.87 77.12 102.87 137.12 162.87 *34.25* *12.87*	25.74 34.25 85.74 94.25 145.74 154.25 *51.49* *4.25*	6.43 53.56 66.43 113.56 126.43 173.56 *12.87* *23.56*	26.56 36.43 83.56 96.43 143.56 156.43 *47.12* *6.43*	8.56 51.43 68.56 111.43 128.56 171.43 *17.12* *21.43*	21.43 38.56 81.43 98.56 141.43 158.56 *42.87* *8.56*	$\sin^{-1}(1/\tan\text{-}\phi) = -12.873$; -167.126 θ_{H3H4} $\cos^{-1}\sin$-17.12 = 107.12 φ_{C4}

Entry	$^3J_{HH}$[Hz][a] Φ[deg] θ_{HnHn+1} [deg]	A	B	C	D	E	F	G	$\varphi_{Cn} = f(\theta_{HnHn+1})$
10	8.8 77.44 -135.7	15.70 44.3 75.7 104.3 135.7 164.3 *31.4* *14.29*	14.29 45.7 74.3 105.7 134.3 165.7 *28.59* *15.70*	28.59 31.40 88.6 91.4 148.6 151.4 *57.19* *1.40*	7.84 52.15 67.85 112.15 127.85 172.15 *15.69* *22.15*	22.15 37.84 82.15 97.85 142.15 157.85 *44.30* *7.84*	7.15 52.84 67.15 112.85 127.15 172.85 *14.30* *22.85*	22.85 37.15 82.85 97.15 142.85 157.15 *45.6* *7.15*	$\tan^{-1}\sin$-77.44 = -44.306; -135.7 θ_{H3H4} $\cos^{-1}\sin$ (-15.70) = 105.7 φ_{C4}
11	8.8 77.44 167.44	17.43 42.56 77.43 102.56 137.43 162.56 *34.87* *12.56*	12.56 47.43 72.56 107.43 132.56 167.43 *25.12* *17.43*	25.12 34.87 85.12 94.87 145.12 154.87 *50.24* *4.87*	8.71 51.28 68.71 111.28 128.71 171.28 *17.43* *21.27*	21.28 38.71 81.28 98.71 141.28 158.71 *42.56* *8.71*	6.28 53.71 66.28 113.71 126.28 173.71 *12.56* *23.71*	23.71 36.28 83.71 96.28 143.71 156.28 *47.43* *6.28*	$\cos^{-1}\sin$-77.44 = 167.44 θ_{H3H4} $\cos^{-1}\sin$ (-17.43) = 107.435 φ_{C4}

*[a] δ[ppm] 2-$D_2$0, ^{13}C 75 [MHz], ^{1}H 400 [MHz].

Tetrahedral angles calculated only from vicinal coupling constant are presented in Table 1 for all possible dihedral angles with negative or positive sign. As reported recently, dihedral θ_{HnHn+1}[deg] and tetrahedral φ_{Cn}[deg] angles calculated from carbon chemical shift δ_{Cn}[deg] are in opposite from the trigonometric point of view, sin *versus* tan functions, for five membered ring [26] comparative to six membered ring [27].

In this case, tetrahedral angles calculated only from vicinal coupling constant, from vicinal angle in close relationship with dihedral angle, results from trigonometric eq. 42, 43 and 9-14 on seven sets angles unit (Table 1), relationship between two pairs of angles A, B with D, E or F, G. For a dihedral angle of 51.56[deg] was calculated a tetrahedral angle of 109.22[deg] in seven set unit, a value somewhat unexpected, probably on corresponding polyhedron [27] an angle of six membered ring. The transformation from U to S gives an angle of 107.18[deg], but also two characteristic angles 34.68 and 55.31[deg] with a vicinal coupling constant of 3.71[Hz], if 55.31 will be considered vicinal angle ϕ[deg], or as results from eq. 9-14, other dihedral angle -34.68[deg] in close relationship with the vicinal angle ϕ 38.44[deg] results from a vicinal constant coupling of 3.1[Hz]. All the equations presented in Table 2 are in close relationships with seven sets angles on one unit.

$$\cos^{-1}\sin(-\phi/2) = \varphi_{Cn} \quad (42)$$

$$\cos^{-1}\sin(-\theta_{HnHn+1}/2) = \varphi_{Cn} \quad (43)$$

Where θ_{HnHn+1} – dihedral angle [deg], ϕ – vicinal angle [deg], tetrahedral angle φ_{Cn} [deg].

The vicinal coupling constant of 3.9[Hz] giving for a dihedral angle θ_{H2H3} of 29.15[deg] a tetrahedral angle φ_{C2} of 104.58, and from transformation S to U a tetrahedral angle of 100.28[deg], for a dihedral angle of -41.12[deg] an angle of 99.43 and other angle on same pair of angles of 101.12[deg], at list for a dihedral angle of -33.91[deg] a tetrahedral angle of 103.04[deg]. In case of dihedral angles θ_{H3H4} with *trans-aa* stereochemistry, tetrahedral angles φ_{C4} are 107.42 for 167.44[deg], 105.7 for -135.7[deg], and 107.12 for -167.13[deg]. In comparation with tetrahedral angles calculated from chemical shift, [26] in this case tetrahedral angle φ_{C2} can be calculated in first case from vicinal coupling constant $^3J_{H1H2}$ or $^3J_{H2H3}$, and tetrahedral angle φ_{C3} from vicinal coupling constant $^3J_{H3H4}$. For example, on two sets angles are found two tetrahedral angles: φ_{C4} and φ_{C3} – 107.41, 102.56[deg].

Table 2. *Conformation simulated with Gausian09W from 3-Sphere dihedral angles θ_{HnHn+1}[deg]* (eq. 9-14) *and corresponding endocyclic torsional angles calculated with eq. 6.*

Entry	$^3J_{HH}$[a] [Hz]	Φ [deg]	θ_{HnHn+1}^{cal}[c] [deg]	θ_{endo} [deg][c]	θ_{HnHn+1}^{G} [deg]	θ_{endo}^{G} [deg]	φ_{Cn}^{gauss} [deg]	l_{CC}^{G} [A^0]	P [deg]	θ_m^b θ_m^c [deg]	Zj[e]	φ_{Cn}^{g} [deg]
							C_1 108.69	C_1C_2 1.5056			0.0446	105.13 (107.5)
1	3.1 3.9 8.8	38.44 60.84 77.44	-52.53 29.15 -167.13	-16.94 7.47 -18.99	-51.90 29.15 -166.1	-17.22 21.75 -18.99	C_2 105.01 C_3 106.85 C_4 108.00	C_2C_3 1.5801 C_3C_4 1.5218 C_4NH 1.543	$_2E$ 342	30.65 7.85	-0.0551 0.0446 -0.0170	102.38 102.40 107.21 (104.2)
							NH 106.7	NHC_1 1.541			-0.0170	109.77
						19.09	C_1 106.61	C_1C_2 1.4967			-0.0599	104.78 (106.6)
2	3.1 3.9 8.8	38.44 60.84 77.44	51.56 -41.12 -135.62	16.63 -10.54 -15.41	51.56 -39.75 -135.6	-2.95 -15.4 25.42 -27.0	C_2 109.25 C_3 106.93 C_4 108.70	C_2C_3 1.5218 C_3C_4 1.5420 C_4NH 1.560	E^0 90	-41.1 -10.5	0.0228 0.0228 -0.0599	104.99 104.19 105.75 (105.3)
							NH 100.7	NHC_1 1.640			0.0740	107.42
							C_1 109.65	C_1C_2 1.532			0.7503[f]	105.13 (107.5)
3	3.1 3.9 8.8	38.44 60.84 77.44	-34.68 29.15 -135.62	-34.5[d] 26.55[d] -9.81[d]	-35.34 29.15 -136.2	-39.44 27.79 -9.818	C_2 107.41 C_3 101.34 C_4 107.33	C_2C_3 1.5218 C_3C_4 1.6588 C_4NH 1.651	$_2E$ 342	30.65 27.91	-0.927[f] 0.7503[f] -0.286[f]	102.38 102.40 107.21 (104.2)
							NH 101.3	NHC_1 1.484			-0.286[f]	109.77

[a] δ[ppm] 2-D_20, ^{13}C 75 [MHz], ^1H 400 [MHz], [b] θ_m – angle of deviation from planarity calculated from 3-Sphere dihedral angle θ_{HnHn+1}[deg], [c] θ_m – angle of deviation from planarity calculated from endocyclic 3-sphere torsional angle θ_{endo}[deg], [d] θ_m – angle of deviation from planarity calculated from Altona torsional angle θ_{endo}[deg] (eq. 3, 5), [e] Zj – out of plane vibrations (eq. 21) calculated from endocyclic 3-sphere torsional angle θ_{endo}[deg] (eq. 6) and phase angle of the pseudorotation P[deg], [f] Zj – out of plane vibrations (eq. 21) calculated from endocyclic Altona's torsional angle θ_{endo}[deg] (eq. 3-5) and phase angle of the pseudorotation P[deg], [g] eq. 28, 29-35.

Two conformations are simulated with Gausian09W in Table 2 using 3-sphere dihedral angles and endocyclic torsional angles calculated with eq. 6. Combination of two consecutive positive or negative dihedral angles are too hard to simulate with VISION molecular models and also with Gausian09W. The angle of deviation from planarity θ_m[deg] with corresponding amplitude q[A^0] are calculated from phase angle of the pseudorotation simulated with Gausian09W. The out of plane vibration Z_i (eq. 21) was calculated from endocyclic torsional angle θ_{endo}[deg] calculated with eq. 6. The angle of deviation from planarity calculated from 3-sphere torsional angles and phase angle of the pseudorotation of 30.65[deg] is expected for Altona formalism, relative to angle for deviation from planarity calculated from endocyclic torsional angle θ_{endo}[deg] of 7.8[deg].

Endocyclic torsional angles calculated with Altona's eq. 3-5 are used for simulation of the conformation of iminocyclitol 1 (Table 1, entry 3), resulting E_2 conformation with θ_m 29.91[deg].

5. Discussion

3-Sphere dihedral angles θ_{HnHn+1}[deg] are used recentry on Altona model as exocyclic angles, and the phase angle of the pseudorotation P[deg] was established with VISION molecular models. The phase angle of the pseudorotation between $^1T_2$ and $_2E$ with P = -24.12[deg] results from Altona model for angles -52.53, 29.67, -168.36[deg], and $_3E$ – $^4T_3$ with P = -143.12[deg] for angles 50.20, -40.98, -135.57[deg]. [10] Exocyclic 3-Sphere torsional angles are considered angles under 180 rule in case of *trans-aa* and 120 rule in case of *trans-ee*. [14] As observation, on VISION molecular models endocyclic torsional angle θ_{endo}[deg] of D-ribitol stereochemistry have same sign as exocyclic 3-Sphere dihedral angles θ_{exo}[deg] in case of *cis*, *trans-aa* and opposite sign in case of *trans-ee* stereochemistry, but don't forgot that VISION molecular models have carbon-carbon bond length and tetrahedral angles frozen.

Conformational results obtained with VISION molecular models are compared with GaussView. 05 program for prediction and visualization of the conformation in Table 2, in first case almost same (entry 1) $_2E$ and in second case different (entry 2) E^0.

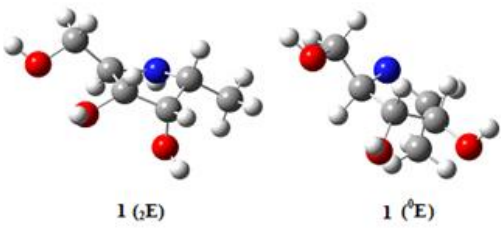

Figure 3. *Simulated Conformation of iminocyclitol 1 with GaussView5.0 (Table 2).*

Remarkably in case of iminocyclitol 1, the *trans-aa* dihedral angles of -135.62[deg] result from eq. 12 is preferred to -167.44[deg] result from eq. 13. on simulation of the conformation with GaussView5.0. Positive dihedral angles of 51.56[deg] and 29.15[deg] for vicinal coupling constants of 3.1 and 3.9[Hz] is too hard to established even with VISION molecular models.

Between the exocyclic dihedral angles and endocyclic torsional angles and implicit tetrahedral angles is almost impossible to obtain accurate correlation with calculated angles. Gausian09W program for prediction and visualization don't corelate tetrahedral angle with dihedral angles as shown in Table 2, but enable a very good visualization of the conformation. Attempts to optimized the conformation with semiempirical PM6 method giving dihedral angles with other vicinal coupling constant $^{3}J_{HnHn+1}$[deg] relative to recorded vicinal coupling constant $^{3}J_{HnHn+1}{}^{exp}$[deg].

Bartenev – Kameneva – Lipanov tetrahedral angle φ[deg] (eq. 29), [17] particularized for all tetrahedral angles (eq. 29-35) are calculated from phase angles of pseudorotation P[deg] simulated with Gausian09W in Table 2. The atom coordinate, the out-of plane vibrations Zj are calculated with Levitt methods (eq. 21). [15]

6. Conclusions

Tetrahedral angles are calculated only from vicinal coupling constant in attempt to corelate the theier relationships with dihedral angles – vicinal angle and vicinal coupling constant. In comparation with tetrahedral angles calculated from carbon chemical shift, tetrahedral angles calculated from vicinal coupling constant are not calculated in opposite with dihedral angles.

The phase angle of the pseudoroataion was simulated with Gausian09W using frozen 3-Sphere dihedral angles and endocyclic torsional angle, but tetrahedral angles are not corelated with dihedral angles in light of 3-Sphere approach. A program for simulation of the endocyclic torsional angles, dihedral angles, carbon-carbon bond lenghts, and tetrahedral angles in function of the vicinal coupling constant or carbon chemical shift is under work.

Abbreviations

NMR	Nuclear Magnetic Resonance

Author Contributions

Petru Filip: Methodology
Carmen-Irena Mitan: Methodology, Writing
Emerich Bartha: Methodology

Conflicts of Interest

The authors declare no conflicts of interest.

References

[1] Kilpatrick, J. E., Pitzer, K. S., Spitzer, R., The termodynamics and molecular structure of cyclopentane, *J. Am. Chem. Soc.* 1947, 2483; https://doi.org/10.1021/ja01202a069

[2] Pitzer, K. S., Donath, W. E., Conformations and strain energy of cyclopentane and its derivatives, *J. Am. Chem. Soc.* 1959, 3213; https://doi.org/10.1021/ja01522a014

[3] Lafferty, W., J., Robinson, D., W., st. Louis, R., U., Russell, J., W., Strauss, H., L., *J. Chem. Phys.* 1965, 42, 2915; https://doi.org/10.1063/1.1703262

[4] Cremer, D., Pople, J. A., General definition of ring puckering coordinates, *J. Am. Chem. Soc.* 1975, 97(6), 1354; https://doi.org/10.1021/ja00839a11

[5] Geise, H., J., Altona, C., Romers, C., The relations between torsional and valence angles of cyclopentane, *Tetrahedron Lett*, 1967, 1383; https://doi.org/10.1016/S0040-4039(00)71589-9

[6] Walczak, D., Sikovski, A., Grzywacz, D., Nawacki, A., Liberek, B., Identification of the furanose ring conformations and the factor driving their adoption, *Carb. Res.* 2023, 526, 108780; https://doi.org/10.1016/j.carres.2013.108780

[7] Painter, W., P., Holman, W., Bush, J. A., Almazedi, F., Malik, H., Eraut, N. C. J. E. M., Morin, J., Szewczyk, L. J., Painter, G. R.., Humansafety, tolerability, and pharmacokinetics of molnupiravir, a novel broad-spectrum and antiviral agent with activity against SARS-CoV-2, *Antimicrob. Agents. Chemother.* 2021, 65, https://doi.org/10.1128/AAC.0428-20 e02428-20

[8] Walczak, D., Nowacki, A., Trzgbinski, D., Samaszko-Fiertek, J., Myszka, H., Sikorski, A., Liberek, B., Conformational studies on *N*-(α-D-glucofuranurono-6, 3-lactone) and *N*-(methyl β-D-glucopyranuronate)-p-nitroanilines, Carb. Res. 2017, 446 - 447, 85; https://doi.org/10.1016/j.carres.2017.05.01

[9] J. B. Houseknecht, C. Altona, C. M. Hadad, T. L. Lowary, Conformational analysis of furanose rings with PSEUROT: parametrization for rings possessing the arabino, lyxo, ribo, and xylo stereochemistry and application to arabino-furanosides, *J. Org. Chem.* 2002, 67, 4647; https://doi.org/10.1021/jo025635q

[10] C.-I. Mitan, E. Bartha, P. Filip, C. Draghici, M. T. Caproiu, R. M. Moriarty, Dihedral angles calculated with 3-sphere approach as integer in conformational analysis on D-, L-ribitol series, *Rev. Roum. Chim.*, 2021, 66, 941; https://doi.org/10.33224/rrch.2021.66.12.07

[11] C. Altona, M. Sundaralingam, Conformational analysis of the sugar ring in nucleosides and nucleotides. Improved method for the interpretation of proton magnetic resonance coupling constants, *J. Am. Chem. Soc.* 1973, *94*, 2333; https://doi.org/10.1021/ja00788a038

[12] Houseknecht, J. B., Altona, C., Hadad, C. M., Lowary, T., Conformational analysis of furanose rings with PSEUROT: Parametrization for rings possessing the arabino, lyxo, ribo, and xylo stereochemistry and application to arabinofuranosides, *J. Org. Chem.*, 2002, 67, 4647; https://doi.org/10.1021/jo025635q

[13] Mitan, C.-I., Bartha, E., Filip, P., Draghici, C., Caproiu, M.-T., Moriarty, R. M., Manifold inversion on prediction dihedral angle from vicinal coupling constant with 3-sphere approach, *Rev. Roum. Chim.* 2023, 68,(3-4), 185; https://doi.org/1-.33224/rrch.2023.68.3-4.08

[14] Bartha, E., Mitan, C.-I., Filip, P., 3-Sphere Torsional Angles and Six Membered Ring Conformation, *American Journal of Quantum Chemistry and Molecular Spectroscopy* 2023, *7*(1), 9. *SciencePG*: https://doi.org/10.116481j.ajqcms.20230701.12

[15] Levitt, M., Warshel, A., Extreme conformational flexibility of the furanose ring in DNA and RNA, *J. Am. Chem. Soc.* 1978, 2607; https://doi.org/10.1021/ja00477a004

[16] H. A. Gabb, S. C. Harvey, Conformational transitions in potential and free energy space for furanoses and 2' deoxynucleosides, *J. Am. Chem. Soc.* 1993, *115*, 4218; https://doi.org/10.1021/ja00063a045

[17] Barlenev, V., N., Kameneva, N., G., Lipanova, A., A., A statistical stereochemical model of the flexible furanose ring, *Acta. Cryst.* 1987, *B 43*, 273; https://doi.org/10.1107/S010876818709788x

[18] F. A. A. M. deLeeuw, C. Altona, Conformational analysis of β-D-ribo, β-D-deoxyribo, β-D-arabinio, β-D-xylo, and β-D-lyxo nucleosides from proton-proton coupling constants; *Perkin Trans 2*, 1980, 1493; https://doi.org/10.1039/P29820000375

[19] Mitan, C.-I, Bartha, E., Filip, P., Caproiu, M.-T, Draghici, C., Moriarty, R. M., Graph Flux Intensity and Electromagnetic Wave on 3-sphere Approach, Science Journal of Chemistry 2023, 11 (6), 212, *SciencePG*: https://doi.org/10.11648/j.sjc.20231106.12

[20] Moriarty, R.-M., Mitan, C.-I., Bartha, E., Filip, P., Naithani, R., Block, T., 3-Sphere approach on 9-O-(10,11-di-O-benzyl-12,14-O-benzylidene-α-D-galactopyrano-syl)-1-butyl-2.3-O-isopropylidene-1,4-dideoxy-1,4-imino-1-N-dehydro-L-ribitol, *American Journal of Quantum Chemistry and Molecular Spectroscopy* 2024, 8 (1), 1; *SciencePG*: https://doi.org/10.11648/ajqcms.20240801.11.

[21] Maksic, Z. B., Randic, M., Carbon-Carbon and Carbon-Hydrogen bond length bond overlap correlations, *J. Am. Chem. Soc.* 1970, 92, 424; https://doi.org/10.1021/ja00705a627

[22] Meyer, R., Lopez, J., C., Alonso, J., L., Melandri, S., Fareno, P. G., Caminati, W., *J. Chemical Physics* 1999, *111*, 7871; https://doi.org/10.1063/1.480122

[23] M. J. Frisch et al., Gausian09W, Revision C.01, Gaussian Inc., 340 Quinnipioc St Bldg 40, Wallingford, CT 06492 USA; www.gaussian.com

[24] VISION molecular models, Darling Models, Inc, P. O. Box 1818, Stow, Ohio 44224 U. S. A.

[25] Mitan, C.-I, Bartha, C. Draghici, M.-T. Caproiu, E., Filip, P., R. M. Moriarty, Hopf fibration on relationship between dihedral angle θ_{HnHn+1}[deg] and vicinal angle ϕ[deg], angles calculated from NMR data with 3-sphere approach and Java Script, Sc. J. Chem. 2022, 10, 21; https://doi.org/10.11648/j.sjc.20221001.13

[26] Mitan, C.-I, Bartha, E., Filip, P., Relationship between tetrahedral and dihedral on hypersphere coordinates, *Rev. Roum. Chim.* 2023, 68(5-6), 261; https://doi.org/10.33224/rrch.2023.68.5-6.09

[27] Mitan, C.-I., Bartha, E., Filip, P., Tetrahedral angles of six membered ring calculated from NMR data with 3-sphere approach, *Rev. Roum. Chim.* 2023, 68(5-6), 269; https://doi.org/10.33224/rrch.2023.68.5-6.1